Building Simulation 2005

Ninth International IBPSA Conference
Montréal, Canada
August 15-18, 2005

MEASUREMENT OF THE THERMAL ENVIRONMENT IN URBAN CANYONS AND PREDICTION BY CFD SIMULATION

Sei Ito[1], Harunori Yoshida[2], Noriko Aotake[3], Kazuya Takahashi[4]

[1]Graduate Student, Dept. of Urban and Environmental Eng., Grad. of Eng., Kyoto University
[2]Prof., Dept. of Urban and Environmental Eng., Grad. of Eng., Kyoto University, Dr.Eng.
[3] The Kansai Electric Power Company Inc, M.Eng.
[4] Central Japan Railway Company, M.Eng.

ABSTRACT

We analyzed the thermal environment within Kyoto city using a numerical model that considers three elements: the unsteady-state heat conduction of building walls and ground surfaces, radiation heat exchange between walls and ground surfaces, and airflow approximated by computational fluid dynamics (CFD). We found that the model accurately simulates the thermal environment accurately within wide urban canyons. However, the various canyon shapes within a city each have unique of thermal characteristics. In order to investigate the influence of canyon shape on the thermal environment, we measured air and surface temperatures in Kyoto city during the summer of 2003. We then compared model predictions with measured air and surface temperatures. The model produced an accurate simulation of the urban thermal environment.

INTRODUCTION

It is well-known that urban air temperature is increasing in cities around the world. The temperature increase is due to diminishing green areas, low wind velocity due to high building density, and the materials used to coat street surfaces. Urban planning requires an understanding of the urban thermal environment and factors that influence heat distribution in such an environment (Williamson *et al*., 2001).

Many studies have undertaken measurement and analysis of the urban thermal environment (H. Yasui *et al*., 2000, A. Yoshida *et al*., 1999). However, many of these studies sought to understand the thermal environment of the city by comparison with the thermal environment of suburban areas. The various shapes of urban canyons range from wide open canyons bounded by buildings of uniform height (Figure 1), to narrow closed canyons bounded by buildings of variable height (Figure 2). It is probable that these canyon have different thermal characteristics. Then it is necesssary to grasp the thermal characteristics to make use of it for improvement of urban thermal environment.

There are also many studies that seek to simulate the urban thermal environment using numerical models. Takahashi *et al.*, (2003) analyzed the thermal environment in Kyoto city using a numerical model that considered three elements: the unsteady-state heat conduction of building walls and ground surfaces, radiation heat exchange between walls and ground surfaces, and airflow approximated by computational fluid dynamics (CFD). The model was able to accurately simulate the thermal environment in wide urban canyons, but some local parts are not accurate enough. And we didn't simulate the thermal environment within narrow urban canyons. Furthermore, there are various canyon shapes within a city and each canyon shape has a unique thermal environment. It is necessary to simulate the thermal characteristics of canyon of various shapes in order to test the accuracy of the model. And if the precision of the model can be proved, using this numerical model, the effect of changing canyon shapes can be investigated in order to improve urban thermal environment at street level.

The aims of this study are: (1) to examine the influence of canyon shape on thermal environment; (2) to test the accuracy of the numerical model by simulating the thermal environment of different canyon shapes and comparing the simulation results with measured data.

MEASUREMENT OF THERMAL ENVIRONMENT

In this section, the measurements of air temperature, ground surface temperature and wall surface temperature are described. The purpose of these measurements is to investigate the influence of canyon shape on thermal environment, to provide boudary conditions for the steady-state CFD simulation, and to provide a test of the simulation results.

Measurement procedure

The measurement site was within central Kyoto city in an area that consists mainly of medium height commercial buildings. Measurements were taken between 1000 hrs and 1600 hrs on 24 August 2003. It

Figure 1 Wide street

Figure 2 Narrow street

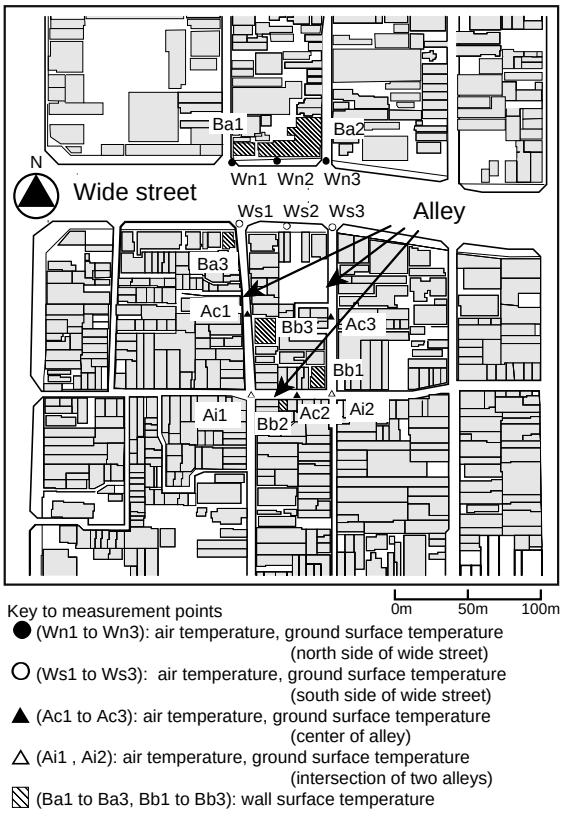

Figure 3 Map of Measurement site

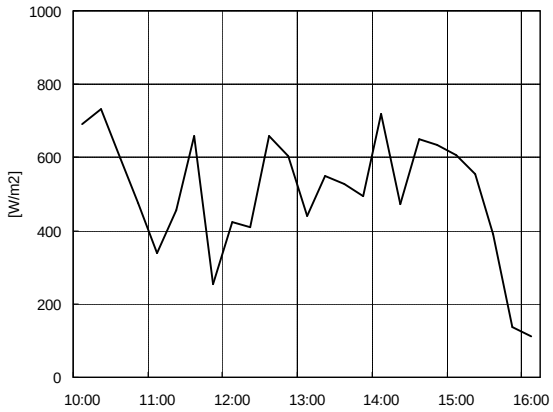

Figure 4 Solar radiation (24 August)

was sunny in measurement period. Air temperature was measured by a thermo recorder at a height of 1.5m, while the surface temperatures of building walls, streets and roofs were measured by a hand-held infrared radiation thermometer. All the measurements were carried out manually at hourly intervals. The locations of measurement sites are shown in Figure 3.

Ba1 to Ba3 and Bb1 to Bb3 in Figure 3 indicate the measurement points of the surface temperature of building walls and roofs. Ba indicates the building which faced a wide street. Bb indicates the building which faced an alley. We measured surface temperatures of the south side and west side walls of Ba1, the east side wall of Ba2, the north side wall of Ba3, the south side and the east side walls of Bb1, the north side wall of Bb2 and the west side wall of Bb3. And we measured surface temperature of the roofs of Ba3 and Bb3. It took 25 minutes to complete each set of measurement.

Wn1 to Wn3 indicate sites of air and ground surface temperature measurement on the north side of a 60m wide street that runs east-west. Ws1 to Ws3 are measurement sites on the south side of the same street. Ac1 to Ac3 are the measurement sites at the center of a 6m wide alley. Ai1 and Ai2 the measurement sites at the intersection of two alleys. It took 20 minutes to complete each set of air and ground surface temperature measurement. In addition, we measured the ground surface temperatures on only the part of sunshine on Wn1 to Wn3 and Ai1 and Ai2 because only sunshine was projected on the north side of wide street and the intersection of two alleys all the time during the measurement; we measured ground surface temperature on only the part of shade on Ws1 to Ws3 because only shade was projected on the south side of wide street all the time during the measurement; we measured the ground surface temperature on both of the part of the sunshine and the shade on Ac1 to Ac3 because both the sunshine and the shade were projected on the ground surface on the center of the alley.

CFD SIMULATION USING MEASURED SURFACE TEMPERATURE AS BOUNDARY CONDITIONS

In this section we describe a steady-state CFD simulation of air temperatures at the measurement sites. Measured surface temperatures are used as boundary conditions in the simulation. The simulation results are compared with measuremed data to check for simulation accuracy.

Model parameters

The *k-e* three-dimensional turbulent flow model (Launder and Kato) (S. Murakami, *et al.*, 2000) is used for the CFD simulation. We assume the fluid to be incompressible (Equation 1), and we solve the simultaneous equations of the laws of conservation of mass (Equation 2), momentum (Equation 3), and energy (Equation 4). The pressure is revised using the SIMPLE method (S. V. Patankar, 1980).

$$r = const. \tag{1}$$

$$\frac{\partial u_i}{\partial x_i} = 0 \tag{2}$$

$$\frac{\partial r u_i}{\partial t} + \frac{\partial r \overline{u_j}\,\overline{u_i}}{\partial x_j} = -\frac{\partial P}{\partial x_i} + \frac{\partial}{\partial x_j} m \frac{\partial u_i}{\partial x_j} - r b g_i (T - T_o) \tag{3}$$

$$\frac{\partial r C_p T}{\partial t} + \frac{\partial u_i C_p T}{\partial x_j} = \frac{\partial}{\partial x_j} K \frac{\partial T}{\partial x_j} + \dot{q} \tag{4}$$

Boundary conditions

Boundary inflow conditions were determined from precalculations as follows. First, a large uniform urban area was formed by connecting a series of model urban areas. Second, inflow conditions were governed by the assumption of the law of exponent in the vertical distribution of horizontal wind velocity and turbulent energy. Third, the vertical distribution of horizontal wind velocity, air temperature and turbulent energy along the flow direction were calculated to determine the point where all distributions became constant. We then adopted these constant distributions as the inflow boundary conditions for the simulation. The turbulence dissipation ratio was calculated from (Equation 5). This value is based on the assumption that generated and dissipated turbulence is balanced at the simulation boundary.

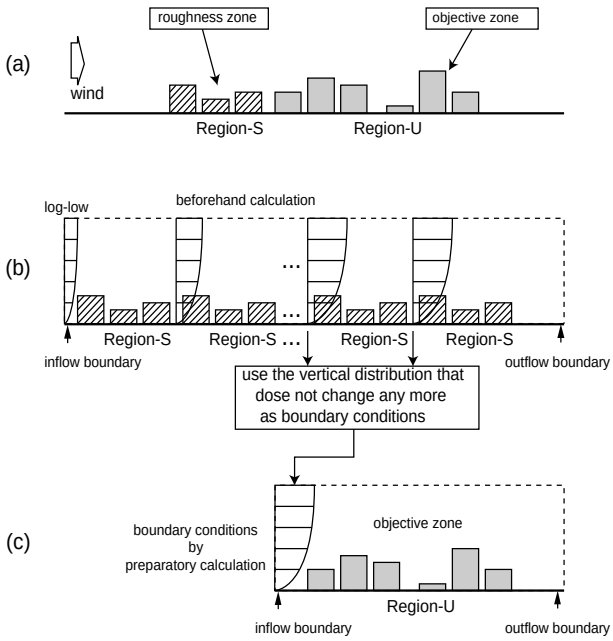

Figure 5 Method to obtain inflow conditions

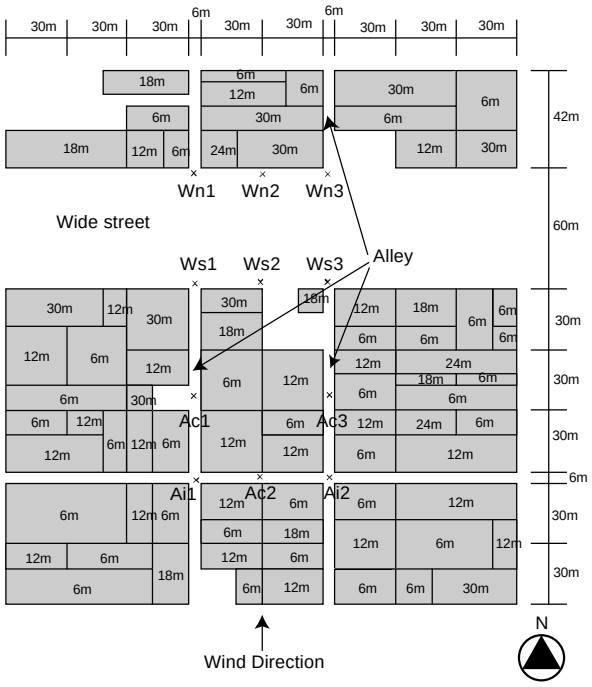

Figure 6 Model of the urban area
(The values inside the cells show the height of the buildings)

Table 1
Surface temperatures used as boundary conditions

		10:00	11:00	12:00	13:00	14:00	15:00	16:00
Buildings faced the wide street	North wall	30.8	32.9	33.4	34.1	35.3	35.9	33.9
	South wall	33.8	37.2	36.4	35.9	41.5	41.6	34.5
	West wall	30.0	32.6	33.1	38.7	42.4	40.9	35.1
	East wall	34.6	35.2	35.2	34.1	36.9	37.9	35.7
	Roof	44.7	47.1	44.7	47.8	50.4	51.5	42.7
Buildings faced the alley	North wall	32.8	34.0	35.0	35.7	37.2	37.2	35.8
	South wall	32.2	34.9	37.3	37.1	38.2	39.3	36.6
	West wall	36.0	33.1	35.0	35.2	36.2	39.4	36.3
	East wall	32.8	35.0	36.5	35.3	36.3	37.1	36.1
	Roof	41.7	43.2	41.4	44.5	45.3	48.4	35.0
The wide street	North side	48.1	44.6	45.6	48.5	47.8	51.9	41.5
	South side	39.3	40.5	40.8	44.4	44.2	42.3	38.2
The alley	Center	38.6	37.1	40.2	44.9	44.7	48.3	40.9
	Crossing	44.3	42.0	43.6	47.3	51.3	51.3	41.1

$$e(z) = C_t^{0.5} k(z) \frac{U_s}{z_z} a \left(\frac{z}{z_z} \right)^{(a-1)} \quad (5)$$

A log-law boundary condition was applied to calculate the stress on surface. The top and sides of the simulation area were assumed to have a free-slip boundary. The heat transfer coefficient was assumed to be 11.6 W/m^2. The air temperature on the top of the model area was fixed at the temperature measured by the Kyoto Meteorological Department .

Simulation details

The model was used to simulate the thermal environment of the measurement site from 1000 hrs to 1600 hrs on 24 August 2003. The size and configuration of the modeled area was replicated from the actual dimensions of the site (Figure 6). The measured surface temperatures were used as boundary conditions (Table 1).

SIMULATION COMBINING RADIATION, CONDUCTION AND CFD

In this section, we describe the unsteady-state CFD simulation that considers three elements: unsteady-state heat conduction of building walls an ground surfaces, radiation heat exchange between walls an ground surfaces, and airflow approximated by CFD.

Calculation Procedure

Calculations were performed as follows (Figure 7).

(1) Initial temperature: The initial surface temperature was calculated on the basis of unsteady-state heat transfer by analysis of 30 days of meteorological measurements of air temperature, solar radiation and long-wave radiation. Air temperature distribution and radiation exchange within the urban space are not considered in our calculation of surface temperature.

(2) Condition at time step *j*: The surface temperature at time step *j* was calculated using the meteorological data at time step *j* and surface temperature at time step *j*–1.

(3) Radiation exchange between surfaces: The heat absorbed by each surface was calculated by considering the mutual reflection of direct sunbeams, sky radiation and long wave radiation between all surfaces. The short wave radiation absorptivity of window glass is assumed to be 0.9 and that of other surfaces is 0.2. The average absorptivity was calculated by assuming that the ratio of windows to wall surface area is 1:4. Long wave absorptivity is assumed to be 0.9.

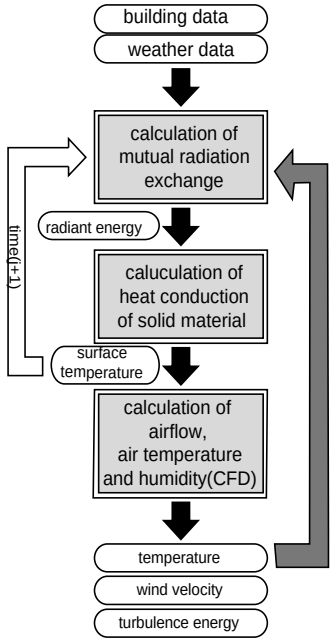

Figure 7 Calculation procedure of the unsteady state CFD simulation.

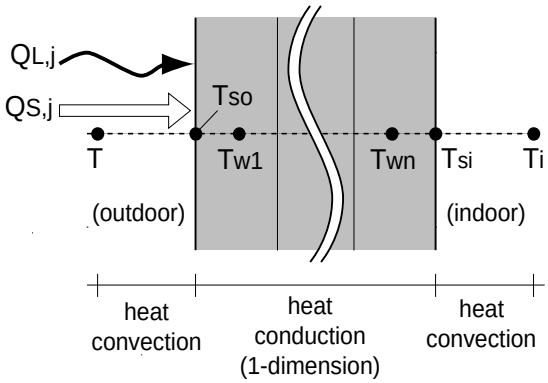

Figure 8 Calculation method of unsteady state heat conduction.

(4) Unsteady-state heat transfer: The temperatures of wall and ground surfaces at time step *j*+1 are calculated by solving the one-dimensional unsteady-state heat conduction equation (Figure 8).

(5) Calculation interval: The time interval of steps (2) to (4) is 1 minute, while air temperature is updated from CFD calculation every 60 minutes.

Simulation details

The calculaton date, location and boundary inflow conditions for the simulation are the same as those described in the previous section. Building walls are composed of mortar (12.5mm thickness), normal concrete (225mm), and mortar (12.5m). The room air temperature is conditioned to 26°C. The ground is composed of asphalt (50mm depth), gravel (150mm)

and soil (800mm). The underside of the ground is assumed to be thermally insulated.

DISCUSSION OF THE MEASUREMENT AND THE SIMULATION RESULTS

In this section, the measurement and simulation results are described and discussed. Symbols used in the presentation of data are listed in Table 2. And the range of the value such as *Ta,a*(M) – *Tw,a*(M) are shown in Table 3 and Table 4.

Table 2 Variables symbol definition for measurement and the simulation results

	faced the Wide Street	faced the Alley
the wall surface temperature	*Tw,w* (the average wall temperature of points Ba1 to Ba3)	*Ta,w* (the average wall temperature of points Ba1 to Ba3)
the roof surface temperature	*Tw,r* (the roof surface of Ba3)	*Ta,r* (the roof surface of Bb3)
	On the Wide street	On the Alley
the ground surface temperatu	*Tw,g* (the average ground temperature of points Wn1 to Wn3 and Os1 to	*Ta,g* (the average ground temperature of points Acn1 to Acn3, Acr1 and
the air temperature	*Tw,a* (the average air temperature of points Wn1 to Wn3 and Ws1 to	*Ta,a* (the average air temperature of points Acn1 to Acn3, Acr1 and
	On the north side of the Wide Street	On the south side of the Wide Street
the ground surface temperatu	*Tn,g* (the average ground temperature of points Wn1 to Wn3)	*Ts,g* (the average ground temperature of points Ws1 to Ws3)
the air temperature	*Tn,a* (the average air temperature of points Wn1 to Wn3)	*Ts,a* (the average air temperature of points Ws1 to Ws3)
	On the center of the Alley	On the intersection of two Alley
the ground surface temperatu	*Tc,g* (the average ground temperature of points Ac1 to Ac3)	*Ti,g* (the average ground temperature of points Ai1 and Ai2)
the air temperature	*Tc,a* (the average air temperature of points Ac1 to Ac3)	*Ti,a* (the average air temperature of points

The variable with subscript (M) indicate the measurement results.
The variable with subscript (S) indicate the simulation results.

Steady-State CFD Simulation results

Steady-state CFD simulation using measured surface temperature as boundary condition was performed in order to check whether the CFD simulation results of air temperature can describe the thermal characteristics of the wide street and the narrow street. In this section we compared the simulated distribution of air temperature with measured distribution.

Table 3 The difference between each variable (steady-state CFD simulation results)

Td [°C]	*x*<*Td*<*X* [°C]	*Td,ave* [°C]
Ta,a (M) – *Tw,a* (M)	*-0.2 < Td <0 .9*	*0.2*
Ta,a (S) – *Tw,a* (S)	*-0.1 < Td <0 .3*	*0.2*
Tn,a (S) – *Tn,a* (M)	*0.3 < Td < 0.8*	*0.6*
Ts,a (S) – *Ts,a* (M)	*0.5 < Td < 1.3*	*1.0*
Tc,a (S) – *Tc,a* (M)	*0.6 < Td < 1.2*	*0.9*
Ti,a (S) – *Ti,a* (M)	*0.2 < Td < 1.1*	*0.5*

Td,ave indicate the average value of Td during the measurement period.

The air temperature within the alley is higher than the air temperature within the wide street in most of measurement period (Figure 9a, Table 3 (*Ta,a*(M) – *Tw,a*(M))). The simulated air temperatures on alley and wide street were also compared (Figure 9a, Table 3 (*Ta,a*(S) –*Tw,a*(S))). And it is found that simulation results accord with the tendency of the measured air temperature.

The simulation results of air temperature on the north and south sides of the wide street are compared with measured results (Figure 9b, Table 3 (*Tn,a*(S) – *Tn,a*(M), *Ts,a*(S) –*Ts,a*(M))). When the simulation results of the air temperature on the south side of wide street were compared with that of the north side of wide street, the air temperature on the south side of wide street cannot be simulated accurately, because this model can be set up boundary inflow wind direction only as northward, southward, westward and eastward, so boundary inflow wind direction of the simulation is set southward, but real wind direction during the measurement was southwest.

The simulation results of air temperature on the center of the alley and the intersection of two alleys are compared with measured results (Figure 9c, Table 3 (*Tc,a*(S) –*Tc,a*(M), *Ti,a*(S) –*Ti,a*(M))). When the simulation results of the air temperature on the center of alley with that of the intersection of two alleys, the air temperature on the center of alley cannot be simulated accurately, because ground surface temperature was set equally, but both the sunshine and the shade were projected on the ground surface on the center of alley, so there was the distribution of ground surface temperature.

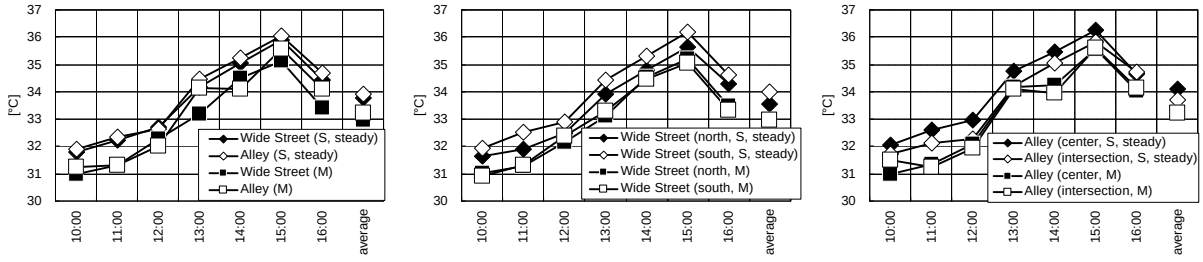

(a) *(b)* *(c)*

Figure 9 Measurement and steady state CFD simulation results of the air temperature

Table 4 The difference between each variable (Unsteady-state CFD simulation results)

Td [°C]	*x*<*Td*<*X* [°C]	*Td,ave* [°C]	*Td* [°C]	*x*<*Td*<*X* [°C]	*Td,ave* [°C]
Tw,w (M) – *Ta,w* (M)	*-0.3 < Td < 0.9*	*0.3*	*Tw,g* (M) – *Ta,g* (M)	*-1.6 < Td < 3.6*	*0.8*
Tw,w (S) –*Ta,w* (S)	*0.4 < Td < 1.2*	*1.0*	*Tw,g* (S) – *Ta,g* (S)	*2.1 < Td < 5.0*	*3.3*
Tw,w (S) – *Tw,w* (M)	*-0.2 < Td < 0.7*	*0.3*	*Tw,g* (S) – *Tw,g* (M)	*-2.7 < Td < 0.1*	*-1.3*
Ta,w (S) – *Ta,w* (M)	*-0.8 < Td < 0.2*	*-0.3*	*Ta,g* (S) – *Ta,g* (M)	*-7.7 < Td < -1.7*	*-4.5*
Tw,r (M) – *Ta,r* (M)	*3.0 < Td < 5.1*	*3.2*	*Tn,g* (M) – *Ts,g* (M)	*3.3 < Td < 10.0*	*6.5*
Tw,r (S) –*Ta,r* (S)	*0.4 < Td < 0.9*	*0.6*	*Tn,g* (S) – *Ts,g* (S)	*1.9 < Td < 9.1*	*4.6*
Ta,a (M) – *Tw,a* (M)	*-0.4 < Td < 0.9*	*0.2*	*Ti,g* (M) – *Tc,g* (M)	*3.8 < Td < 8.8*	*5.6*
Ta,a (S) – *Tw,a* (S)	*0.0 < Td < 0 .3*	*0.2*	*Ti,g* (S) – *Tc,g* (S)	*1.6 < Td < 4.4*	*3.2*
Tn,a (S) – *Tn,a* (M)	*0.0 < Td < 1.2*	*0.5*	*Tc,a* (S) – *Tc,a* (M)	*-0.1 < Td < 1.2*	*0.7*
Ts,a (S) – *Ts,a* (M)	*0.4 < Td < 1.6*	*0.9*	*Ti,a* (S) – *Ti,a* (M)	*-0.1 < Td < 0.9*	*0.5*

Unsteady-State CFD Simulation results

Measured surface temperatures are used as boundary condition in steady-state CFD simulation. Since no surface temperature is available for predicting environment of given urban area, we have developed a new numerical model to predict the surface temperature, which can simulate it by combining CFD calculation with surface radiation exchange calculation and unsteady-state heat transfer calculation of walls and ground surface. In this section we discuss whether the model simulated distribution of surface temperature and air temperature can match the measured distributions.

The wall surface temperatures of buildings faced the wide street is higher than that of the alley in most of measurement period (Figure 10a, Table 4 (*Tw,w*(M) –*Ta,w*(M))). The simulated wall surface temperature of buildings faced the wide street and the alley were compared (Figure 10a, Table 4 (*Tw,w*(S) –*Ta,w*(S))). It is found that simulation results accord with the tendency of the measured wall surface temperatures.

The simulation predictions of wall surface temperatures are compared with measured results (Figure 10b,c). We conclude that the model is able to accurately predict changes in wall surface temperature over time.

The roof surface temperatures of buildings faced the wide street is higher than that of the alley in most of measurement period (Figure 11a, Table 4 (*Tw,r*(M) – *Ta,r*(M))). The simulated roof surface temperature of buildings faced the wide street and the alley were compared (Figure 10a, Table 4 (*Tw,r*(S) –*Ta,r*(S))). It is found that simulation results do not accord with the measured roof surface temperatures, because material value of roof that is different from the real ones was set up.

The ground surface temperatures on the wide street is higher than that of the alley in most of measurement period (Figure 12a, Table 4 (*Tw,g*(M) –*Ta,g*(M))). The simulated ground surface temperature on the wide street and the alley were compared(Figure 12a, Table 4 (*Tw,g*(S) –*Ta,g*(S))). And it is found that

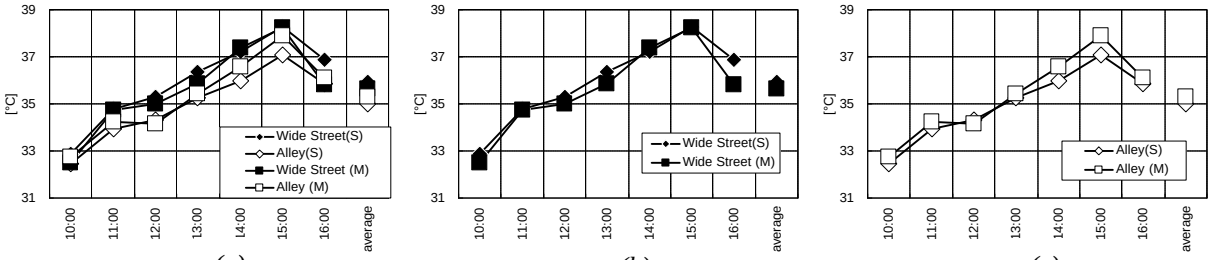

Figure 10 Measurement and simulation results of the wall surface temperature

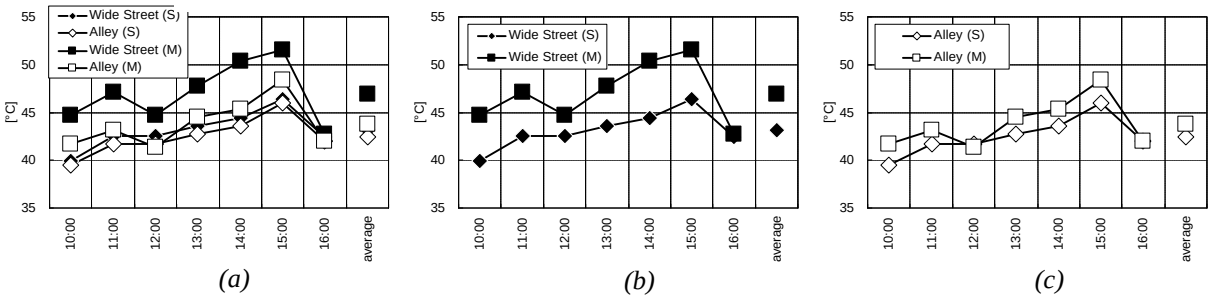

Figure 11 Measurement and simulation results of the roof surface temperature

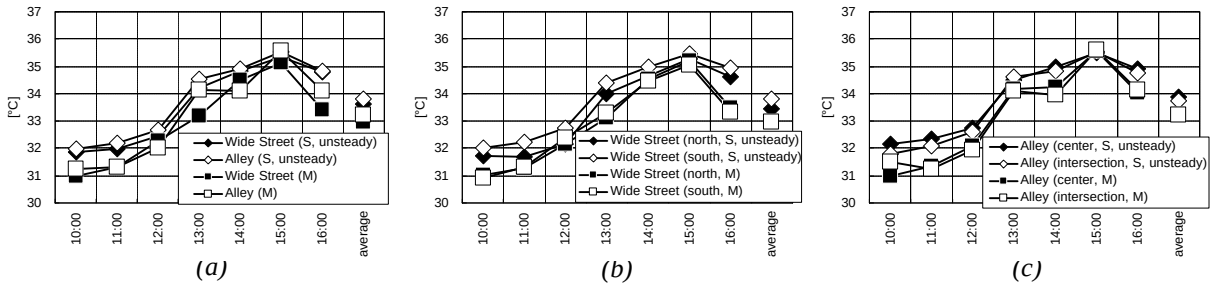

(a) *(b)* *(c)*

Figure 13 Measurement and unsteady state CFD simulation results of the air temperature

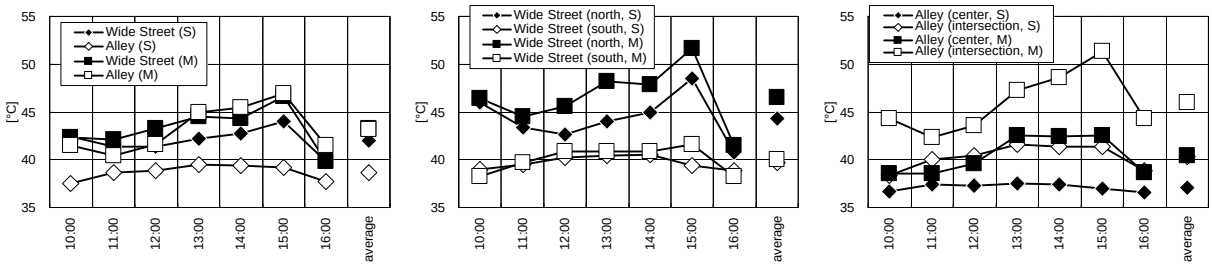

(a) *(b)* *(c)*

Figure 12 Measurement and simulation results of the ground surface temperature

simulation results accord with the tendency of the air temperature. But the difference between *Ta,g*(S) and *Ta,g*(M)(*Ta,g*(S) – *Ta,g*(M)) range from –7.7 to –1.7°C, and the model is not able to accurately predict the ground surface of the alley, because the model calculated sky view factor (SVF) at each mesh (minimum mesh size is 6m×6m), so the model is not be able to simulate the real sunshine and shade projection. But the measured ground surface temperatures were calculated considering the sunshine projection on the ground using the simulation results of the SVF.

The air temperature within the alley is higher than the air temperature within the wide street in most of measurement period (Figure 13a, Table 4 (*Ta,a*(M) – *Tw,a*(M))). The simulated air temperatures on the alley and the wide street were also compared (Figure 13a, Table 4 (*Ta,a*(S) –*Tw,a*(S))). It is found that simulation results accord with the tendency of the air temperature.

CONCLUSION

Measurement of the urban thermal environment within Kyoto city was carried out in order to examine the influence of canyon shape on the thermal environment. And the measurement results were compared with simulation results. The following conclusions can be summerized.

(1) The steady-state and unsteady-state CFD simulations of air temperature predict that *Ta,a*(M) is higher than *Tw,a*(M), and this prediction is confirmed by measurement data. The absolute value of the difference between predicted air temperatures and measured data are within 1.6°C. Therefore the numerical model provides accurate predictions of air temperature.

(2) The unsteady-state CFD simulation of wall, roof and ground surface temperatures correctly predicted that ground surface temperatures within a wide street, and the surface temperature of buildings that face a wide street, are higher than equivalent temperatures within a narrow alley.

(3) The absolute value of the difference between predicted wall surface temperatures and measured data are within 1.0°C for all data points. We conclude that the wall surface temperature can be accurately simulated.

(4) The roof surface temperature could not be accuratelly simulated because the roof material used in the simulation is different from the roof material on the buildings.

(5) The differences between *Tw,g*(S) and *Tw,g*(M) range from –2.7 to 0.1°C, while the differences between *Ta,g*(S) and *Ta,g*(M) range from –7.7 to –1.7°C. The ground surface temperature within the alley cannot be simulated as accurately as the surface within the wide street because the ground surface of the alley contains areas of both sunshine and shade.

NOMENCLATURE

C_p : Specific heat of air [J/kgK]

C_t : Model constant [-](=0.09)

g_i : Acceleration [m/s^2]

k : Turbulent energy [m^2/s^2]

K : Coefficient of heat conduction [J/msK]

P : Atomosphere pressure [N/m^2]

$\dot{q}$: Heat generation [J/m^{3}s]

t : Time [sec]

T : Air temperature [K]

T_0 : Basic air temperature [K](=303)

u_i : Velocity [m/s]

U_s : Wind velocity on reference height [m/s]

x_i : Space co-ordinate [m]

z : Height [m]

z_s : Reference height [m]

a : Exponential order[-](=0.2)

b : Coefficient of volume expansion [l/K]

e : Dissipation rate of turbulence energy [m^2/s^3]

m : Coefficient of viscosity [kg/ms]

r : Density of air [kg/m^3](=1.176)

REFERENCES

K. Harayama, and S. Yosida: Numerical study based on unsteady radiation and conduction analysis, Prediction of outdoor environment with unsteady coupled simulation of convection, radiation and conduction -Part 1-, J. Archit. Plann. Environ. Eng., AIJ, No. 556, 99-106, June 2002

S. Murakami, *et al.*,: Computational Environment Design for Indoor and Outdoor Climates, University of Tokyo Press, 2000

K. Takahashi, Yoshida, H. *et al.*,: Heat Flux Measurement of Urban Boundary Layers in Kyoto City and its Prediction by CFD Simulation, Building Simulation, 8th International Conference, pp.1265-72, Aug. 2003

Williamson, T. J. and Evyatar Erell: Thermal performance simulation and the urban microclimate: measurement and prediction, Seventh Internal IBPSA Conference, Rio de Janeiro, Brazil, August 13-15, 2001

H. Yasui, J. Tsutsumi *et al.*,: Field measurement of temperature and humidity distributions downtown in Naha, Summaries of Technical Papers of Annual Meeting, AIJ, D-1, pp.655-56, 2000

A. Yoshida, Y. Omoto: Field measurement of local air temperature in town area, Summaries of Technical Papers of Annual Meeting, AIJ, D-1, pp.699-700, 1999

S. V. Patankar: Numerical heat transfer and fluid flow, Hemisphere Publishing Corporation, 1980